New approach on Dynamic Voltage Restorer Topology, Testing and Control Techniques

Bruno Costa, *IST Student* and J. Fernando Silva, *Associate Professor of Power Electronics*
Department of EEC, IST, Lisbon, Portugal, September 2007

***Abstract* – This paper presents the structure and control of a Dynamic Voltage Restorer (DVR) that injects the needed voltage to mitigate voltage sags in order to eliminate the sag ominous effect in the critical load. The DVR has the secondary winding of the transformer placed in series with the distribution line and, its control system, has to act the most quickly has possible when a voltage sag is detected to make sure that the load isn't affected by this kind of disturbances.**

The control of the DVR includes: 1) one internal loop to control the power inverter AC currents using αβ space vector modulation (SVM); 2) one external loop that uses a linear proportional integral (PI) controller for the AC voltages, which are controlled acting in the references of the internal current control and 3) one discrete DC capacitor voltage controller that injects current pulses to keep constant the voltage value of the capacitors of the Energy Storage System.

These controls are tested using MatLab/Simulink in diverse situations. Obtained results and options taken in the project are discussed.

I. Introduction

Nowadays, voltage sags are considered the biggest problem in power quality issues. These disturbances are sudden reductions of the voltage values understood between 90% and 1% of the nominal voltage in a distribution feeder for a reduced time. Most of them doesn't last more than 500 ms and have a remaining voltage higher than 50% [1]. The most common causes are [2]:

- defects (short circuits);
- procedures in the distribution network and operation errors;
- bad operation of consumer equipment;
- switching of major loads (starting motors or switching on transformers that demand high currents of the network).

Voltage sags or dips can cause major problems for several production processes that require high power quality standards. Mainly, continuous manufacture processes have really high vulnerability to voltage sags. Even small dips in the distribution network can cause several hours of lost production due to product damage, disrupted process, contamination and time lost to restart the process.

With the increasing economic necessity to compensate voltage sags, the Dynamic Voltage Restorer (DVR) comes as a good solution to mitigate this problem. The main purpose of the DVR is to detect the voltage sag and react as quickly as possible to restore the correct voltages making the critical load immune to this type of disturbance. During the voltage sag, the DVR has to deliver enough energy to the load to maintain his nominal voltage.

Before installing a DVR, it is necessary to monitor the network to have a background on the most typical problems that may affect the facility. This technology is recognized as the most effective equipment that can be used to counter the voltage sag problem.

II. DVR Topology

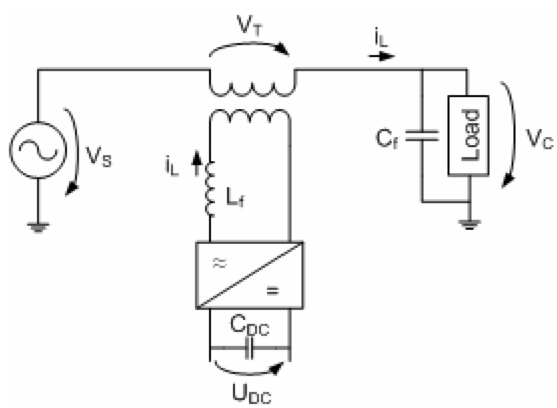

Figure 1 - Simplified DVR Topology.

The DVR, here considered, is a three-phase system. For simplicity, Figure 1 represents the single-phase equivalent of the system.

In order to compensate the voltage sag in the distribution line, it's necessary to have an energy storage system. We consider a capacitive storage (ultracapacitors are good candidates) rated according the depth and time span of the sag we want to protect from, since sag probability and damage are enough to make the DVR economically viable. Between the network and the critical load the DVR puts the transformer secondary winding (Figure 1). In the primary winding, there is a voltage source inverter with three control loops. A LfCf filter is designed to remove switching high frequency current and voltage harmonics.

The DVR system will withstand several tests, like various types of voltage sags and non-linear loads, to evaluate the performance of the designed control loops.

III. Mathematical Modeling

The two sets of semiconductors in the same arm of the three-phase voltage source inverter (Figure 2) must be in complementary states. This represents a restriction imposed by the need to prevent short circuits on the DC side. Thus, the state of the devices of each arm k (k=A, B, C) can be represented by the switching variable γ_k [5].

$$g_k = \begin{cases} 1 \rightarrow S_{1k}ON & S_{2k}OFF \\ 0 \rightarrow S_{1k}OFF & S_{2k}ON \end{cases} \tag{1.1}$$

These states can be represented in the αβ vector referential through the application of the Concordia matrix (1.5). To generate the AC waveforms (1.2) (1.3) (1.4), the inverter changes from one state to another, as imposed by the control technique [7].

$$V_{AN} = \frac{(2g_A - g_B - g_C)U}{3} \tag{1.2}$$

$$V_{BN} = \frac{(2g_B - g_A - g_C)U}{3} \tag{1.3}$$

$$V_{CN} = \frac{(2g_C - g_B - g_A)U}{3} \tag{1.4}$$

$$\begin{bmatrix} V_a \\ V_b \\ V_0 \end{bmatrix} = \sqrt{\frac{2}{3}} \begin{bmatrix} 1 & -\frac{1}{2} & -\frac{1}{2} \\ 0 & \frac{\sqrt{3}}{2} & -\frac{\sqrt{3}}{2} \\ \frac{1}{\sqrt{2}} & \frac{1}{\sqrt{2}} & \frac{1}{\sqrt{2}} \end{bmatrix} \cdot \begin{bmatrix} V_{AN} \\ V_{BN} \\ V_{CN} \end{bmatrix} \tag{1.5}$$

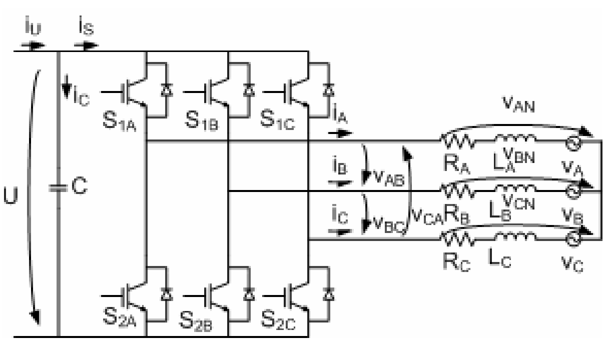

Figure 2 – Voltage Source Inverter.

The dynamic behavior of the system (Figure 2), where R_k, L_k and V_k represent the network voltages and impedances, can be obtained applying Kirchhoff's Laws. To design the controller it is mandatory to obtain a simple model, but at the same time useful and reliable. The time dependent equations that represent the AC currents and DC voltage dynamics are:

$$\frac{di_k}{dt} = \frac{v_{kN} - R_k i_k - v_k}{L_k} \tag{1.6}$$

$$\frac{dv_C}{dt} = \frac{i_U - i_S}{C} \tag{1.7}$$

Later it will be necessary to consider the capacitor (Figure 1) in parallel with each load phase to design the AC voltage control loop. The capacitor is used to filter out the voltage high frequency harmonics.

IV. Current Control using αβ Space vector modulation (SVM)

Several modulation techniques exist to define the switching variables γ_k which drive the power semiconductors. As power converters are inherently non-linear, variable structure systems, it makes sense the application of a control such as sliding mode [6]. Since the AC currents show first order behavior relatively to the input control, the sliding surface is simply the error e_{ij} between the reference current and the measured current ($e_{ij} = i_{jref} - i_j$) in the αβ frame ($j=\alpha,\beta$). Since the converter can only present 8 output voltage vectors (Figure 3) and only two currents are independent, in order to quantify the current error, two three-level relays are used. According to the output of the two relays, the switching strategy chooses an αβ vector able to decrease the current error, ensuring the sliding mode stability condition $e_{ij}\, de_{ij}/dt<0$.

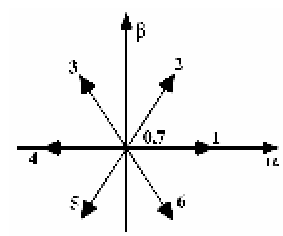

Figure 3 – αβ vectors.

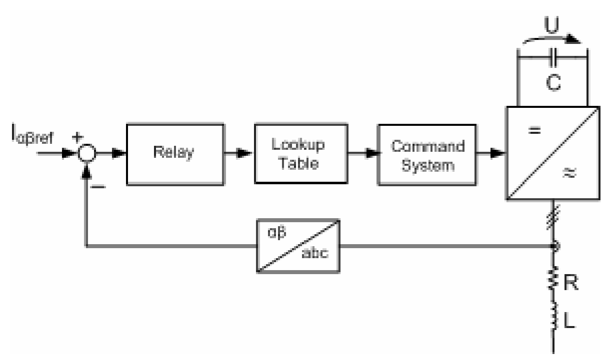

Figure 4 - Current control loop.

From the quantified three discrete values (δ=-1, 0, 1) of the current errors e_{ij}, the switching law can be used to built Table 1, which defines which αβ vector is used for every possible combination of errors.

Table 1 – αβ vectors for the 3^2 state control.

	$d_b = -1$	$d_b = 0$	$d_b = 1$
$d_a = -1$	5	4	3
$d_a = 0$	5/6	0/7	2/3
$d_a = 1$	6	1	2

For some combinations of errors there exist two possible vectors. This leaves room for some improvement that can be made by minimizing the switching frequency. For example, if vector 5 is being applied and (δ_α,δ_β) change to (0,-1), then vector 5 continues to be applied. Also, if vector 6 is being applied and (δ_α,δ_β) changes to (0,-1), then vector 6 continues to be applied. This applies also to vectors 2 and 3. Another improvement can be made with vectors 0 and 7 by knowing the previously used vector and minimizing the number of switchings needed to obtain the null vector.

A three level relay can be obtained through the sum of two different relays, each of them with different hysteresis windows. The width of the hysteresis window is related with the AC current ripple. The tighter the window gets, less ripple is in the output current. However, there is a substantial increase on the switching frequency. Therefore, the inductor will be calculated assuming a switching frequency f_s near to 4 kHz (1.8).

$$L = \frac{U}{4\Delta I_n f_s} \qquad (1.8)$$

V. AC Voltage Control

Capacitor C_f and inductor L_f (Figure 1) form an LC low-pass filter. By choosing the filter cut-off frequency f_c, we are able to calculate the capacitor value (1.9). The f_c frequency has to be a decade below the switching frequency f_s and, if possible, a decade higher than the frequency of the fundamental harmonic (50Hz). The value of the capacitor can also be given as a function of the ripple DV (1.10) [5].

$$f_C = \frac{1}{2p\sqrt{L_f C_f}} \qquad (1.9)$$

$$C_f = \frac{U_{DC}T^2}{48\Delta V} \qquad (1.10)$$

To control the AC voltages, it is used a linear control technique that takes advantage of the internal sliding mode current control loop. The voltage controller defines the reference current for the internal current controller, in order to obtain the desired AC voltage. Therefore, it needs saturation blocks to limit the short circuit AC currents of the converter. This method is an indirect form of voltage control with a double feedback system [10]. The dynamic response of the current control has to be faster than the dynamic response of the voltage control for a proper functioning.

Considering the load as a resistive circuit, we have a generic phase equivalent as shown in Figure 5.

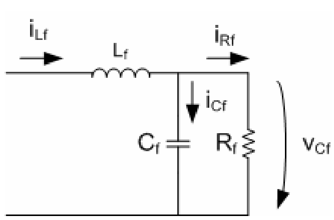

Figure 5 - Generic phase at the end of the inverter.

Applying the Kirchhoff's laws to the circuit, (1.11) is obtained.

$$\frac{dv_{Cf}}{dt} = \frac{i_{Lf} - i_{Rf}}{C_f} \qquad (1.11)$$

It is possible to represent this system on a state-spaced averaged model and apply the Concordia and Park transformation to change the abc referential to the αβ referential or to the dq referential. A non linear but time invariant model is obtained, because of the existing coupling between the V_{Cfd} and V_{Cfq} variables, as shown in (1.12) (1.13) [10].

$$V_{Cfd}(s) = \frac{1}{s}\left(wV_{Cfq}(s) + \frac{i_{dref}(s)}{C_f} - \frac{i_{Rfd}(s)}{C_f} \right) \qquad (1.12)$$

$$V_{Cfq}(s) = \frac{1}{s}\left(-wV_{Cfd}(s) + \frac{i_{qref}(s)}{C_f} - \frac{i_{Rfq}(s)}{C_f} \right) \qquad (1.13)$$

To be able to use a linear controller, to process the error between the referenced voltage and the measured voltage, it is necessary to have a linear model. To make the necessary decoupling of the two variables a variable change is applied, (1.14) (1.15) [10].

$$V_{Cfd}(s) = \frac{1}{sC_f}\left(h_{dref}(s) - i_{Rfd} \right) \qquad (1.14)$$

$$V_{Cfq}(s) = \frac{1}{sC_f}\left(h_{qref}(s) - i_{Rfq} \right) \qquad (1.15)$$

Where h_{dref} and h_{qref} are defined by equations (1.16) and (1.17).

$$h_{dref}(s) = wC_f V_{Cfq}(s) + i_{dref} \qquad (1.16)$$

$$h_{qref}(s) = -wC_f V_{Cfd}(s) + i_{qref} \qquad (1.17)$$

Now, it is possible to design a closed loop linear voltage control. This voltage control is based on a compensator which has to be designed to ensure zero steady state errors. Therefore, proportional or proportional derivative compensators are not suitable. Only proportional integral (PI) controllers can guarantee zero steady state errors, together with acceptable rise times and good stability margin [4].

The voltage control block diagram, using a PI controller C(s), is represented in Figure 6.

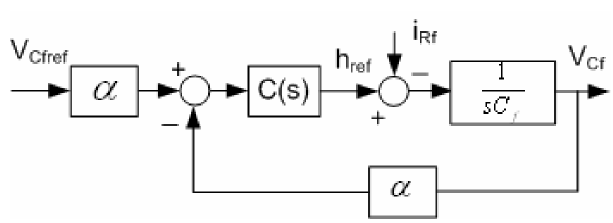

Figure 6 - Block diagram of the linear system.

The block diagram is valid in the dq reference frame, and allows the calculation of the PI parameters. To eliminate the restriction of the previously considered resistive load, the current flow into the load is considered a system perturbation. The proportional and integral gains are designed for a proper response of the system to this perturbation. The denominator of the closed loop transfer function is equivalent to a second order system. Imposing the damping factor, ξ, equal to 0,707 and the natural frequency 10 times lesser than the switching frequency, the PI gains can be obtained [9].

However, given the load disturbance, the gains can be tuned applying the Ziegler-Nichols rules. These rules are based on a trial with the objective to obtain acceptable transient response with the commitment between quickness and relative stability [12].

The complete block diagram of the voltage control, together with the current control loop is represented in Figure 7.

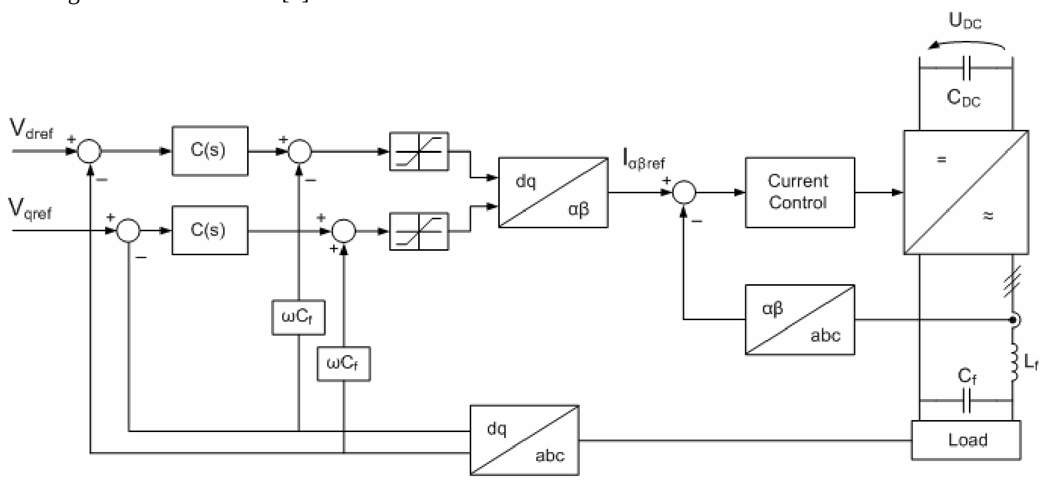

Figure 7 - Complete block diagram of the AC voltage control.

VI. DC Voltage Control of the energy storage capacitor

This DC voltage controller must deliver energy to the energy storage capacitor without affecting the controlled AC voltage at the critical load. This represents a huge restriction, since it is impossible to transfer active power from the AC voltages without somewhat disturbing them. Nevertheless, there exists a -10% margin in the voltage amplitude, that by standards is not a voltage sag, and the critical load must be designed to withstand. Some DC energy storage controllers based on Park transformations affect the critical load in order to charge the energy storage system. So, to charge this system, we have to transfer energy in small periods of time for the voltage and current waveforms don't get affected.

The control presented in this paper is a discrete voltage controller where, through the measurement of the currents that passes in the transformer, chooses the right vector to be applied (transferring energy to the capacitor), or applies zero vectors (no energy transfer). The energy transfer only happens during brief instants but is being repeated. This originates a current pulse train to charge the energy storage system. The architecture of this control is represented in Figure 8.

The current detection is based on equation (1.18). Knowing that a period in a balanced three-phase system can be divided in six sections, it's easy to choose the right vector to choose in order to increase U_{DC}.

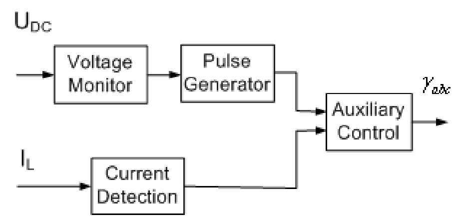

Figure 8 - Architecture of the discrete voltage control.

$$i_C \approx -\left(g_A i_A + g_B i_B + g_C i_C\right) \tag{1.18}$$

Thus, we establish a correspondence between γ_k and the positive/ negative current values using the function (1.19).

$$\begin{cases} i_k > 0 \rightarrow 1 \\ i_k < 0 \rightarrow 0 \end{cases} \tag{1.19}$$

A DC voltage monitor block updates the control when there is need to charge the energy storage system. The auxiliary control block decides between the vector coming from the Current Detection block and vector 0. The time duration of the imposed vector is determined by the pulse generator. The duty cycle and the current pulse period determine the restitution rate of the voltage value. A low restitution rate is needed in order to maintain almost undisturbed voltage and current waveforms in the critical load.

VII. AC Detection and Synchronization Technique

The DVR dynamic response must be as quick as possible, which means that the voltage sag must be detected promptly. In this case, the only information needed in the control is the start and end of the voltage sag. A comparison between the amplitude of the norm of the αβ vectors and 90% of their value is used for sag detection, since other techniques would lead to worst response times [15].

The angular position *q* of the network must be known to perform the AC voltages control. Like the sag detection system, the system to synchronization with *q* has to be quick and immune to noise effects, to minimize the degradation of the DVR effectiveness. Through the acquisition of the voltage values of the network, it's possible to build a synchronizer as shown in Figure 9. It is based on the Concordia Transformation matrix (1.5) and uses a Low-Pass Filter to reduce the noise. The fast response of this synchronizer is always dependent of the delay imposed by this filter. After calculating the norm of the αβ vectors, we are able to obtain the sin(θ) and cos(θ) needed to synchronize. To eliminate the delay introduced by the filter, it is possible to use trigonometric formulas, (1.20) [11].

$$\begin{aligned} \sin(x \pm y) &= \sin(x)\cos(y) \pm \sin(y)\cos(x) \\ \cos(x \pm y) &= \cos(x)\cos(y) \mp \sin(x)\sin(y) \end{aligned} \quad (1.20)$$

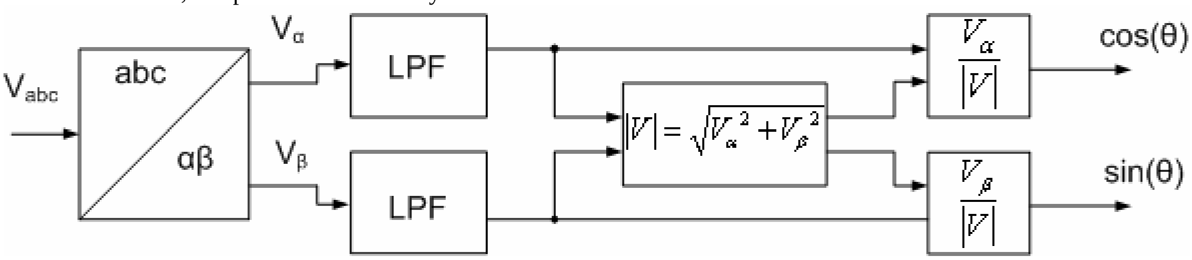

Figure 9 - Synchronizer.

VIII. Results

A. Sliding mode AC current control.

The first results to be shown are the operation of the non-linear sliding mode AC current control on a simple inverter model. The nominal current is 30A and the objective is to verify if the AC currents of the inverter track the reference currents imposed by the control. As Figure 10 shows, the currents follow the references. Table 1 with improvements is used, because it leads to fewer commutations, although the switching frequency is not the same for all the 3 converter legs.

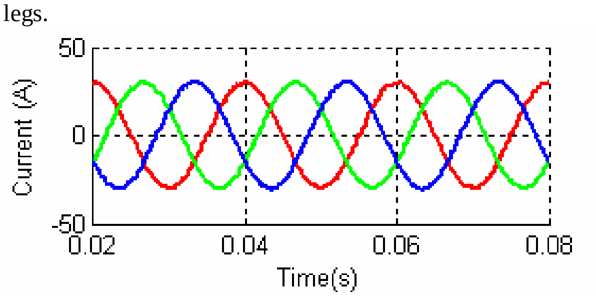

Figure 10 - AC currents on the inverter.

B. PI AC Voltage Control.

The linear PI AC voltage control makes use of the internal sliding mode current control, as explained before. The results presented are from the complete model of the DVR. A simple voltage divider is used to simulate a voltage sag in the distribution line as shown in Figure 11. The voltage sag has a depth of 50%, two 50Hz cycles duration, and is almost instantaneous. This does not correspond to the reality because voltage sags have there own transient response. Nevertheless, this event is near the worst case scenario, the interruption of the power supply. The response of the DVR is represented in Figure 12. As seen, the voltage in the critical load does not show any disturbances, which means the AC voltage controllers are able to follow their references. The response time is very short. This is visible in Figure 15 that presents the response of the DVR, in one of the phases, and the 90% lower limit of the nominal voltage.

Figure 13 represents the voltage in the secondary winding of the transformer. With nominal network voltage, in spite of the application of vector 0, the winding voltage is not null due to the internal parasitic impedances of transformer and switches. The current in the load is represented in Figure 14 being the critical load basically resistive.

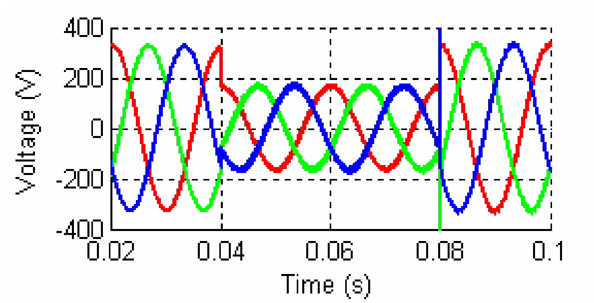

Figure 11 - Voltage on the distribution line.

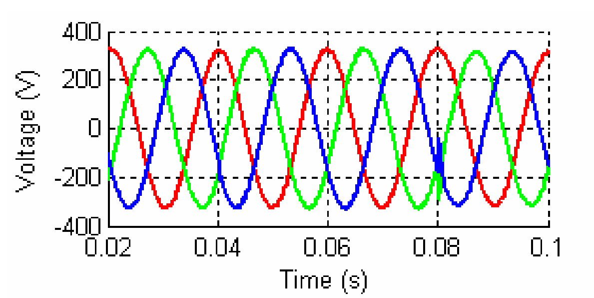

Figure 12 - Voltage in the critical load.

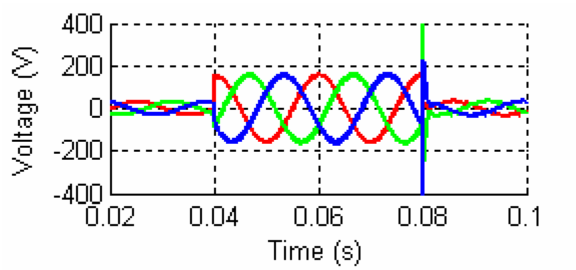

Figure 13 - Voltage on the secondary winding of the transformer.

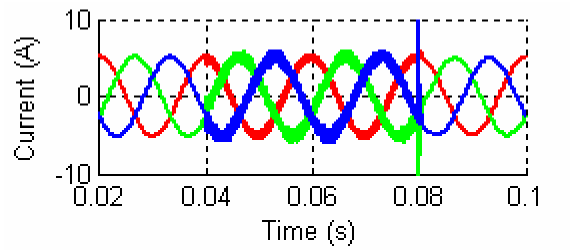

Figure 14 - Current in the critical load.

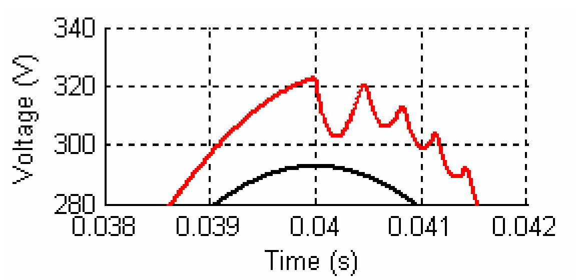

Figure 15 - Zoom of the time response of the DVR.

In the case of a complete interruption of the power supply, being necessary to protect the critical load from this kind of events, the DVR designed is equally valid, provided that the necessary energy is stored. Also, it might be necessary to increase the value of U_{DC} for a proper response of the DVR.

The results shown assume the energy storage system is charged. As said, the DVR can be operated to charge the energy storage system. By doing that, it is not necessary to use a charging unit making the system much more attractive in an economic point of view. However, an "always on" mode, without charging the capacitor, brings other advantages as a better operation with non-linear loads (Figure 16 and Figure 17).

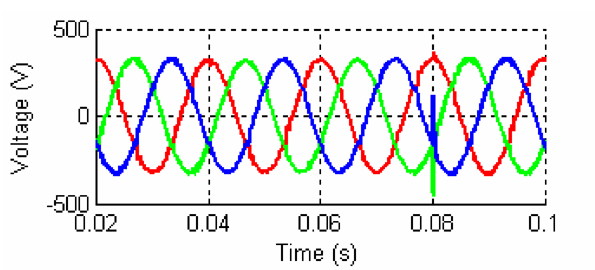

Figure 16 - Voltage on the non-linear load.

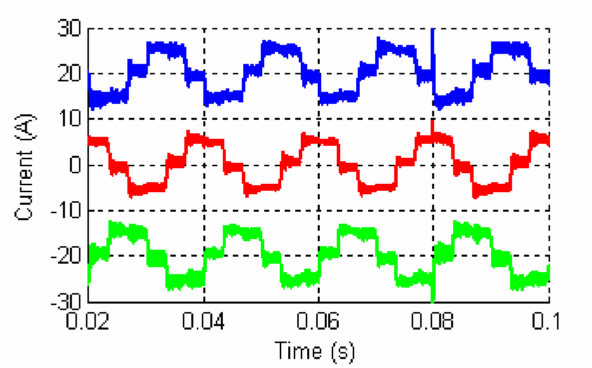

Figure 17 - Current on the non-linear load.

The very fast response of the DVR to the voltage sag was only possible after fine tuning through the application of the Ziegler-Nichols rules.

The designed control system assumes that the network is a balanced and symmetrical system. But in some cases, it's necessary to protect the critical load from asymmetrical sags. Despite the fact that the control system was not designed for this kind of events, it still has a good response for sags with a depth of 33,3%. Above that value, voltage oscillations appear.

The synchronizer imposes another restriction in the DVR control. The system is dependent on the information from the network voltages making it impossible to know the angular position in case of interruptions or extremely deep sags. One possible solution would be to disaggregate the synchronizer during the sag. The reference would be generated based on the last information known.

C. DC voltage control.

This type of control can benefit from the easy change of restitution rate by changing the pulse rate. Even for high restitution rates it's easy to compensate the reduction of the voltage amplitude on the load with the inclusion of transformer between the DVR and the load. The charge time of the energy storage system also depends on the amplitude of the current that flows on the transformer winding. Obviously, it's only possible to apply this control if the AC voltage control is on stand-by mode. In case of being used a independent charging unit, this control can be also applied or choose a PWM modulation. The pulses have a 2% duty cycle and a frequency 30 times higher than the network frequency. This will cause a 2% reduction of the voltage value in the load. Although the voltage has a 10% margin, it isn't a good idea to use it all because, in contrast with the frequency, the amplitude of the voltage in the network suffers from great fluctuations. The charge/discharge of the energy storage system is represented in Figure 18.

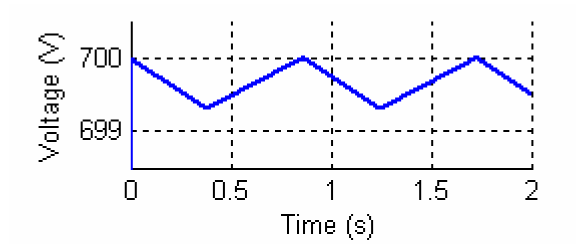

Figure 18 - Charge/discharge of the energy storage system.

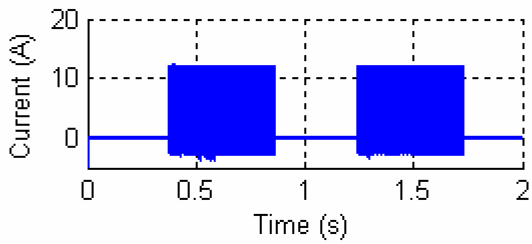

Figure 19 - Current impulses.

As it can be verified, it's possible to maintain a certain value of voltage in the capacitor with extreme precision. With these parameters and amplitude of the current the restitution rate it's of 1,45V/s. The decrease of 2% of voltage amplitude in the load is visible in Figure 20. This means that this control can cause a disturbance ("flicker") in the load but with minor values.

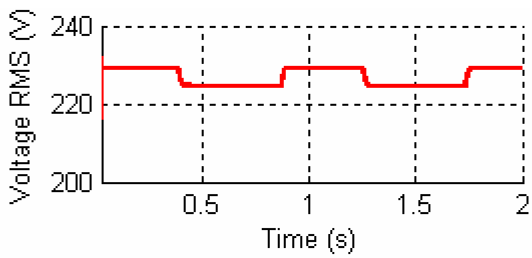

Figure 20 - Voltage RMS in the load.

IX. CONCLUSION

The development of this work and analysis of the results allows us to conclude that the designed system is comparable to any DVR present in the market. Surely the short response time to the voltage sag is the strongest point of this control. Since the response time is very fast, any load is protected from this kind of disturbance.

The sliding mode non-linear current control seems to be appropriate because we're in the presence of a non-linear system. The use of all the available vectors reduces the commutations in the converter, but the switching frequency is not the same for all the 3 converter legs. Later on, it was verified that the linear voltage control tends to even this difference between the commutation frequencies in the three arms of the inverter.

In the linear AC voltage control, the application of a PI controller and decoupling proves itself to be appropriate and with great potential. The controller gains were tuned with the Ziegler-Nichols Rules. The use of a stand-by control or an always on control depends on the conditions present when we are faced to sags. If the load is mainly a non-linear load, it isn't viable to use a stand-by control. If the conditions are favorable for a stand-by control, the use of the discrete voltage control excuses the charging unit. The biggest flaw in this control is asymmetrical sags, needing future studies in this area. Both detection and synchronization techniques show to be efficient and accurate.

The discrete voltage control permits to rapidly charge the energy storage system without affecting the critical load.

X. REFERENCES

[1]. Oliver Suter, Michael Buschmann, Gerhard Linhofer, Philippe Maibach, "Voltage Source Converter based Power Quality Solutions", Asia Pacific Regional Power Quality Seminar, 28-31 March 2005, Marriot Putrajaya, Malaysia.

[2]. J. Fernando Silva, "Sistemas de Armazenamento de Energia", Apresentação, Maio 2006.

[3]. Humberto Jorge, "Qualidade de Energia – Cavas de Tensão, Interrupções", Apresentação, Fevereiro 2004.

[4]. Muhammad H. Rashid, "Power Electronics Handbook", Academic Press, 2001

[5]. J. Fernando Silva, "Sistemas de Energia em Telecomunicações", Textos de Apoio, Março 2006

[6]. J. Fernando Silva, "Electrónica Industrial", Fundação Calouste Gulbenkian, Lisboa, 1998

[7]. Gil Marques, "Dinâmica das Máquinas Eléctricas", Textos de Apoio, Abril 2002.

[8]. João Santana e Francis Labrique, "Electrónica de Potência", Fundação Calouste Gulbenkian, Lisboa, 1991

[9]. Isabel Lourtie, "Sinais e Sistemas", Escolar Editora, 2002

[10]. João Dionísio Barros, "Conversores Multinível: Comando e Controlo por Computador", Dissertação de Mestrado, Outubro 2005.

[11]. Nuno Silva, "Controlo das Potências Activa e Reactiva Fornecidas à Rede Eléctrica por Conversores CC/CA Fontes de Tensão", Dissertação de Mestrado, Agosto 2004, Porto

[12]. Eduardo Morgado, "Controlador PID", Apontamentos de Controlo, Outubro 2003

[13]. www.abb.com

[14]. www.sand.com

[15]. Chris Fitzer, Mike Barnes and Peter Green, "Voltage Sag Detection Technique for a Dynamic Voltage Restorer", IEEE Transactions on Industry Applications, vol. 40, no. 1, January/February 2004.

[16]. S. S. Choi, B. H. Li and D. M. Vilathgamuwa, "Design and Analysis of the Inverter-Side Filter Used in the Dynamic Voltage Restorer", IEEE Transactions on Power Delivery, vol. 17, no. 3, July 2002

[17]. Hyosung Kim, Sang-Joon Lee and Seung-Ki Sul, "A Calculation for the Compensation Voltages in Dynamic Voltage Restorers by use of PQR Power Theory", IEEE, 2004

[18]. Jing-Chung Shen and Huann-Keng Chiang, "PID Tuning Rules for Second Order Systems", Department of Electrical Engineering, Yunlin, Taiwan.

[19]. Neil Woodley and Trevor Holden, "Field Experience with the New Platform-Mounted DVR", IEEE, 2000

[20]. John Godsk Nielsen, Michael Newman, Hans Nielsen, Frede Blaabjerg, "Control and Testing of a Dynamic Voltage Restorer (DVR) at Medium Voltage Level", IEEE Transactions on Power Electronics, vol. 19, no. 3, May 2004

[21]. Changjiang Zhan, Vigna Kumaran Ramachandaramurthy, Atputharajah Arulampalam, Chris Fitzer, Stylianos Kromlidis, Mike Barnes and Nicholas Jenkins, "Dynamic Voltage Restorer Based on Voltage-Space-Vector PWM Control", IEEE

Transactions on Industry Applications, vol. 37, no. 6, November/December 2001

[22]. Mahinda Vilathgamuwa, Ranjith Perera and S. S. Choi, "Performance Improvement of a Dynamic Voltage Restorer With Closed-Loop Load Voltage and Current-Mode Control", IEEE Transactions on Power Electronics, vol. 17, no. 5, September 2002

[23]. P. Boonchiam and N. Mithulananthan, "Dynamic Control Strategy in Medium Voltage DVR for Mitigating Voltage Sags/Swells", International Conference on Power System Technology, 2006